ELSEVIER

PII: S0032-3861(97)10255-5

Influence of composition and morphology on rheological properties of polyethylene/polyamide blends

J. Huitric[a],*, P. Médéric[a], M. Moan[a] and J. Jarrin[b]

[a]*Laboratoire de Rhéologie, I.U.P. Génie Mécanique, Université de Bretagne Occidentale, 6, avenue Victor le Gorgeu, 29285 Brest Cedex, France*
[b]*Institut Français du Pétrole, B.P. 311, 1-4 avenue Bois Préau, 92506 Rueil-Malmaison, France*

The effects of composition and resulting morphology on rheology of blends of polyethylene and polyamide 12, two immiscible polymers having the same Newtonian viscosity but different elasticity, were studied in the whole range of volume fraction. The composition dependence of zero shear rate viscosity η_0 and first normal stress difference N_1 show a positive deviation from the additivity law: η_0 and N_1 increase gradually at low and moderate volume fraction of the dispersed phase, but remain almost constant in the phase inversion region. The variation of zero shear rate viscosity has been analysed, in relation to morphology observations, by an emulsion model as developed by Oldroyd in the case of droplet-type morphology and by a layer model which takes into account the simultaneous presence of droplets and fibres when the morphology is partially fibrillar. If the volume fraction of the dispersed phase is not too low, the first normal stress difference is proportional to shear rate, in agreement with the prediction of Doi–Ohta theory, as a result of morphology modifications during flow. The linear viscoelastic behaviour has been analysed using Palierne's model and the interfacial tension between the two polymers has been determined by fitting the dynamic moduli with this model. © 1998 Elsevier Science Ltd. All rights reserved.

(Keywords: PE/PA12 blend; morphology; rheology)

INTRODUCTION

Modification of industrial polymer properties is currently obtained by blending immiscible polymers in the melt[1]. Blend properties depend on constituent polymers, on the heterogeneous morphology formed during the processing, and on agents often added to blends of homopolymers to enhance the compatibility. Addition of an elastomer to a thermoplastic matrix significantly improves its impact strength[2]. Barrier properties are generally obtained by a lamellar dispersion of an impermeable phase, e.g. a polyamide, in a polyethylene matrix[3]. The morphology obtained, either nodular, fibrillar, lamellar or co-continuous, is mostly formed by blending in the melt, and therefore largely depends on the rheological behaviour of the constituents and the blend's mechanical and thermodynamic conditions. In fact, the final morphology is determined by the level of local stresses encountered in the mixing of polymers, the blend composition, the interfacial tension and the viscoelastic properties of the components. On the other hand, rheological behaviour of the blend in the melt, often different from that of individual phases, is strongly related to this morphology. Hence, it is important to properly control this inter-relationship for obtaining the required morphology for a particular application.

The objective of this study is to contribute to a better understanding of the influence of the dispersed phase and its morphology on the rheological properties of blends; this will be achieved by measuring not only the steady shear

---

* To whom correspondence should be addressed

viscosity but also the dynamic viscosity, as well as the steady first normal stress difference over the entire range, from zero to one, of volume fraction of dispersed phase. To show in the best way the influence of the dispersed phase, we have chosen to prepare blends with various morphologies from polymers as close as possible in their rheological behaviour. To this end, a polyethylene/polyamide 12 (PE/PA12) pair was selected with a zero shear viscosity ratio almost equal to 1 and an interfacial tension high enough to clearly show compatibilizer influence in our future work. Moreover, PE and PA12 samples were chosen to provide optimum accuracy in the measurements of rheological parameters of interest in this work. In other words, these samples, which have almost the same viscosity, are Newtonian over a wide range of shear rates, and both have a long relaxation time, but short enough for the low frequency terminal zone to be observed in the commonly accessible frequency range.

EXPERIMENTAL

Materials

Blends were prepared from two commercial polymers, a low density linear PE (FLEXIRENE FG 20) and a PA12, respectively supplied by Enichem and Elf Atochem. *Table 1* shows some of their characteristics including the number average and the weight average molecular weights, denoted M_w and M_n.

The blends have been made, with volume fractions of PA12 ranging from 0 to 100%, by mixing the components in a Haake mixer (Rheocord E U 5). The blending conditions

Table 1 Characteristics of materials used in this study

Material	M_w	M_n	Melting point (°C)
PE	140 000	37 000	121
PA12	48 800	25 500	170

were the same for all blends: temperature 195°C; rotational speed of the blades 32 rpm, that is a shear rate of about $100\ \text{s}^{-1}$. Mixing time corresponds to the obtaining of a constant torque on the blades, that is about 5 min, then the blends were quenched in cold water for 2 or 3 min. After cryo-grinding, the blends were squeezed between plates in a heating press under 20 MPa at 195°C. Because of their hygroscopic nature, PA12 and PE/PA12 blends were dried for 4 h at 85°C in a vacuum oven before experiments.

Rheological measurements

Steady shear viscosity, first normal stress difference and dynamic viscoelasticity data were obtained using a Rheometrics Dynamic Analyser (RDA II) with parallel plate geometry (25 mm diameter and 2 mm spacing). All experiments were carried out at a temperature of 195°C. This value, higher than the melting temperature of each polymer, was chosen to allow adequate duration of the experiments without noticeable degradation. Yet samples were tested under a continuous nitrogen purge in the case of PA and of blends having a relatively high fraction of PA. All data on dynamic moduli correspond to a strain amplitude (4%) for which the response is linear viscoelastic.

Morphology

The morphology of the blends were observed, by using a scanning electron microscope (SEM) on cryo-fractured surfaces.

RESULTS AND DISCUSSION

Rheological characterization of pure polymers

Figures 1 and 2 show for PE and PA12 respectively, the variation of the viscosity (η), and of the first normal stress
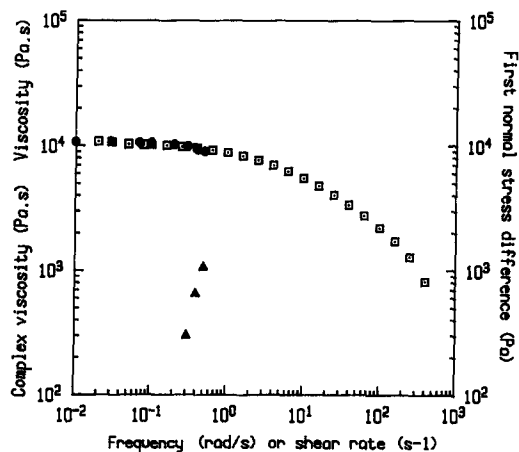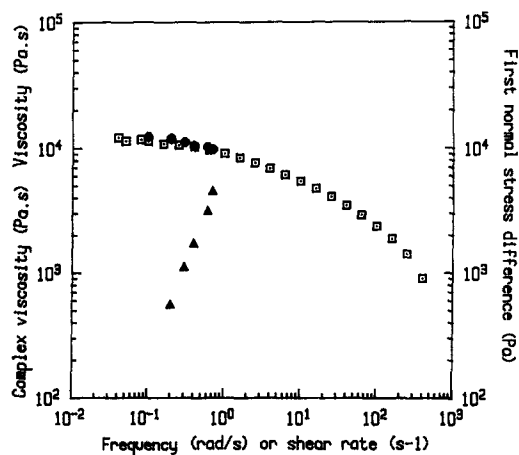

Figure 2 Shear rate dependence of viscosity (•) and first normal stress difference (▲), and frequency dependence of complex viscosity (□) for PA12

Figure 3 Frequency dependence of loss modulus (•) and storage modulus (■) for PE

Figure 1 Shear rate dependence of viscosity (•) and first normal stress difference (▲), and frequency dependence of complex viscosity (□) for PE

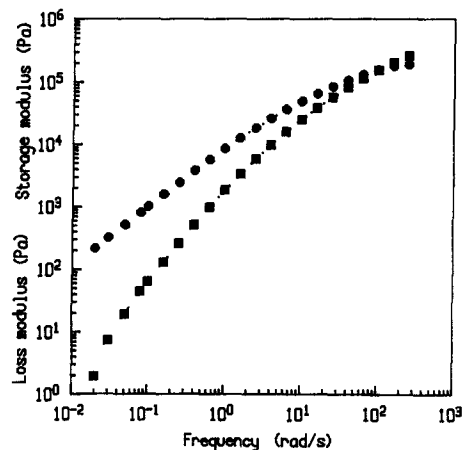**Table 2** Rheological characterisatics of pure polymers

Polymer	η_0 (Pa s)	N_1 (Pa) at $\dot\gamma = 2 \times 10^{-1}\ \text{s}^{-1}$	G' (Pa) at $\omega = 2 \times 10^{-1}\ \text{rad s}^{-1}$
PE	10 750	200	195
PA12	11 400	500	300

difference N_1 *versus* shear rate $\dot\gamma$ as well as the complex viscosity $|\eta^*|$ *versus* frequency ω. For each polymer, one can observe that the low shear rate viscosity plateau broadly spans up to about $2 \times 10^{-1}\ \text{s}^{-1}$ and that the Cox–Merz rule is quite well verified. Both observations allow the determination of the zero shear viscosity η_0 with satisfactory accuracy. As shown in *Table 2*, these two polymers have approximatively the same zero shear viscosity (η_0(PA12)/η_0(PE) = 1.06) at a temperature of 195°C. Yet the first normal stress difference measured in the near-Newtonian regime ($N_1 \propto \dot\gamma^2$) shows a significant variation from PE to PA12. Therefore, it seems that the polyamide presents a higher elasticity than the polyethylene (N_1(PA12)/N_1(PE) = 2.5) in the range of shear rates used (see *Table 2*).

Figures 3 and 4 show, for each polymer, data of the storage modulus G' and loss modulus G''. They indicate that in the range of accessible frequencies the terminal zone is clearly displayed, i.e. $G' \propto \omega^2$ and $G'' \propto \omega$ at lowest frequencies. Moreover, as indicated in *Table 2*, the storage modulus for PA is slightly higher than that of PE in the terminal zone. This is in at least qualitative agreement with what was observed for the first normal stress difference.

Blend morphology
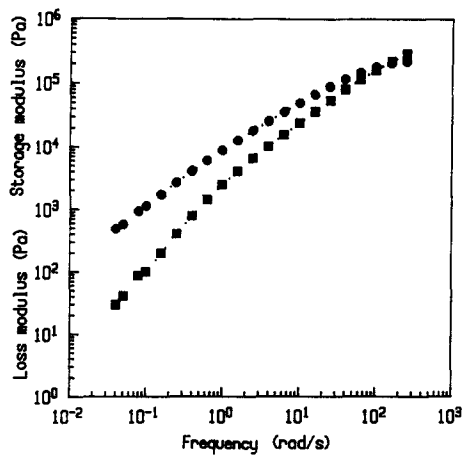
Besides the influence of composition and of blending and

Figure 4 Frequency dependence of loss modulus (•) and storage modulus (■) for PA12

Table 3 Description of PE/PA12 blend morphologies

Φ (%PA12)	Observations
5, 10, 15, 20 and 30	Nodular morphology without contact (region 1)
45 and 50	Fibrillar morphology (region 2)
75, 80, 90 and 95	Nodular morphology without contact (region 3)

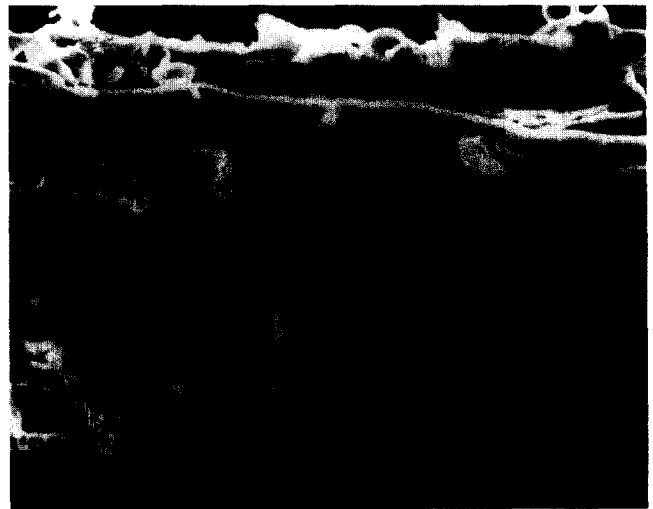**Figure 6** SEM of a cryo-fractured 70/30 PE/PA12 blend: nodular morphology

Figure 7 SEM of a cryo-fractured 50/50 PE/PA12 blend: fibrillar morphology
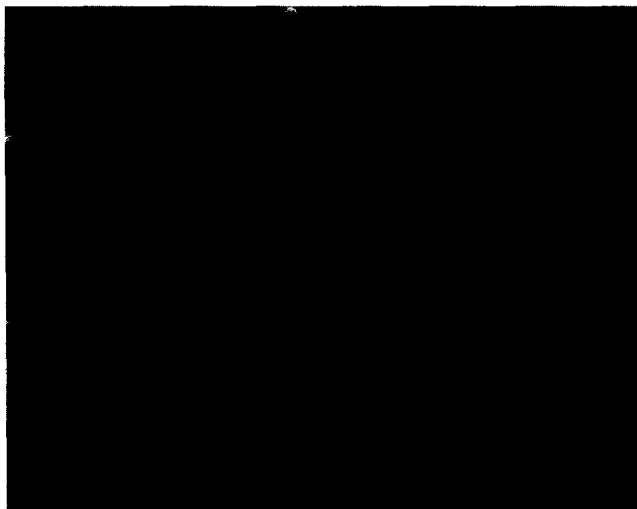

Figure 5 SEM of a cryo-fractured 95/5 PE/PA12 blend: nodular morphology

pressing conditions, the morphology and the final size of the dispersed phase result from a balance between various forces: viscosity forces which tend to deform a droplet, together with interfacial tension forces and also those related to the droplet elasticity which try to resist the deformation. In fact, during mixing, and for low fractions of the dispersed phase at least, equilibrium particle size results from continuous breakup and coalescence of the dispersed particles. As the fraction of the dispersed phase is increased, there is an increase in coalescence, so that the drops become progressively larger and then deform into fibres[4–6].

Morphological observations of PE/PA12 blends are summarized in *Table 3*. The composition dependence for the blend morphology, as the volume fraction of PA12 increases from 0 to 100%, is characterized by three regions

separated by two transition zones. In region 1, microscopy reveals a nodular morphology: polyamide particles grow in size as PA12 volume fraction increases (*Figures 5 and 6*). In region 2, a fibrillar phase appears (*Figure 7*). This roughly corresponds to phase inversion, that is, to the presence of co-continuous phases. After phase inversion, we can once more observe a nodular dispersion now made of polyethylene particles (*Figure 8*). In this third region, in accord with the behaviour in the first one, nodule size grows along with polyethylene content in the blend. However, two differences are observed when comparing the two regions: first, PE nodules are more bulky than PA12 nodules for the same volume fraction; and second, region 3 is less extensive than region 1. The objective of this study is not to explain the observed morphology, however we think that these two results can be related to the relative elasticity of the constituents and may be partially supported by the analysis of Starita[7]. That author considers that the relative elasticity affects only the strain recovery. For a viscosity ratio of the components close to 1 and N_1 (dispersed phase) > N_1 (matrix), a spherical dispersion is expected due to strain recovery. On the contrary, when N_1 (dispersed phase) < N_1 (matrix), there is no strain recovery and hence a fibrillar
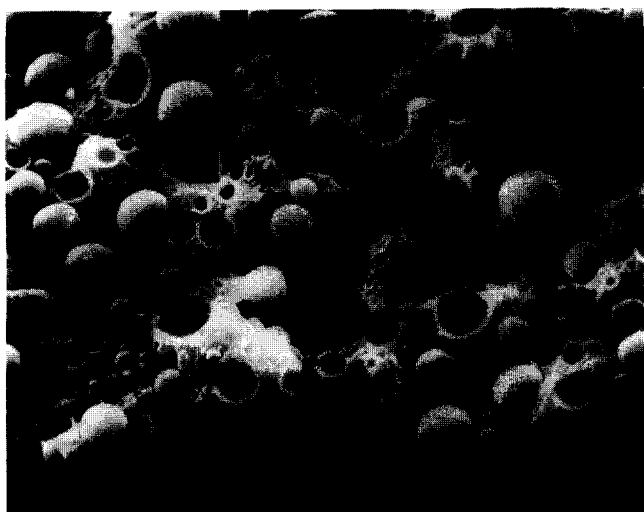
Figure 8 SEM of a cryo-fractured 20/80 PE/PA12 blend: nodular morphology

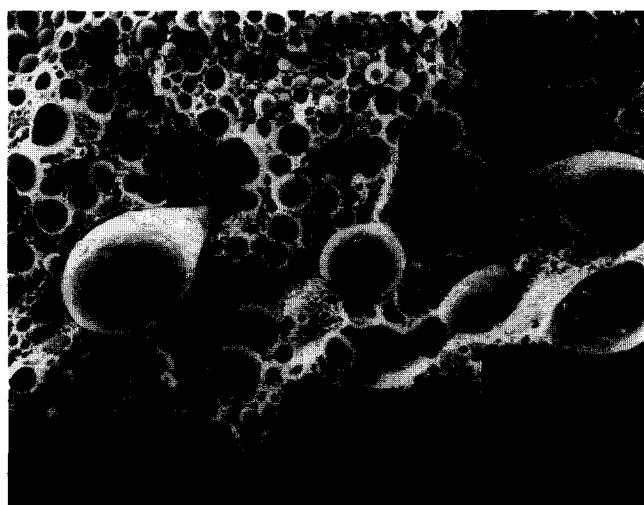**Figure 9** SEM of a cryo-fractured 55/45 PE/PA12 blend: droplets and fibres

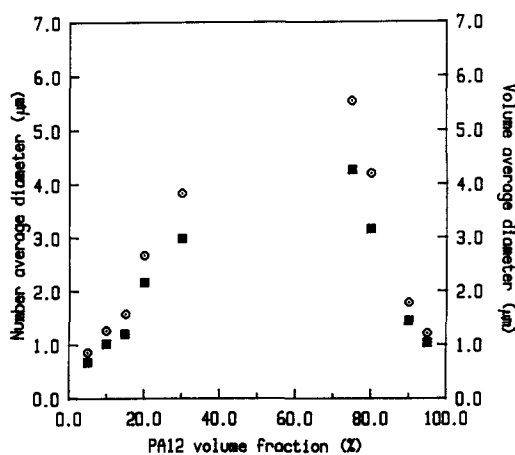**Figure 10** SEM of a cryo-fractured 60/40 PE/PA12 blend: presence of dumbbell-shaped bodies

Figure 11 Variation of the number average diameter (■) and the volume average diameter (○) with PA12 volume fraction
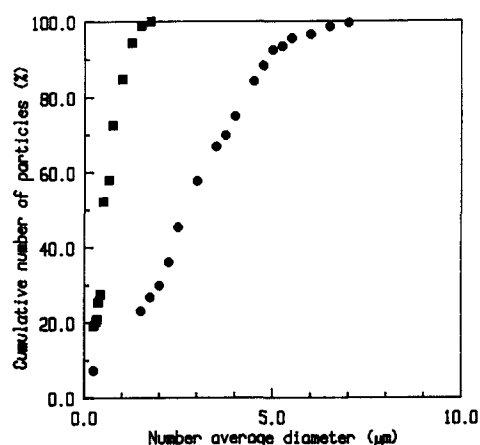

Figure 12 Minor phase size distribution curves for PA12 dispersed in PE, for PA12 volume fractions 5% (■) and 30% (•)

morphology is preserved. According to this reasoning, the lower elasticity of PE, N_1(PE) $<$ N_1(PA12), could therefore account for an earlier transition zone when it represents the dispersed phase (region 3). However, this interpretation should be considered cautiously, since we are not able to measure first normal stress difference at shear rates that are encountered in the mixing chamber ($\dot{\gamma} = 100$ s^{-1}), and also we cannot ignore a partial relaxation of fibrils during blend quenching. This could account for a type of morphology, consisting of fibrils and also of nodules, shown in *Figure 9*. Both transition zones, which are characterized by contact interactions between particles, are not well-defined. For instance, at a 40% volume fraction of PA12, we observe the presence of nodules, but also that of elongated or dumbbell-shaped bodies (*Figure 10*).

The image analysis provides the number-average diameter d_n of the minor phase (regions 1 and 3). In both regions, d_n increases linearly with the volume fraction of the dispersed phase, as shown in *Figure 11*. However, it can be noticed that, for the same volume fraction of the minor phase, d_n is rather larger (1.5 times) for PE nodules in a PA12 matrix than for PA12 nodules in a PE matrix. A possible interpretation in terms of relative elasticity of the components was provided in the paragraph above. The observed particle sizes can be approximately described by a log-normal distribution, as shown in *Figure 12*; these
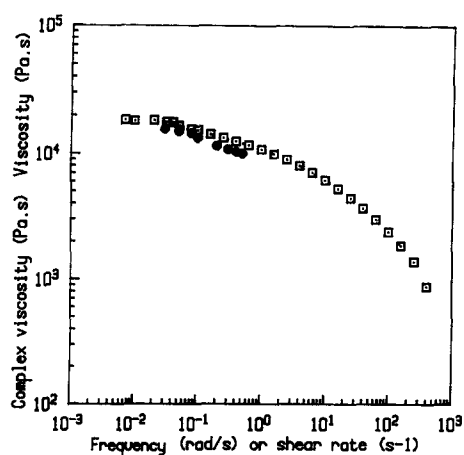
Figure 13 Shear rate dependence of viscosity (•) and frequency dependence of complex viscosity (□) for 70/30 PE/PA12 blend

Figure 14 Volume fraction dependence of zero shear viscosity for PE/PA12 blend

distribution curves indicate a low polydispersity in the size of the minor phase, which is practically independent of the volume fraction, at least for PA12 dispersion in PE. Yet we can notice a very slight increase of size polydispersity *versus* volume fraction for PE dispersion in a PA12 matrix, as shown previously for PE/PA[6] and PP/PC[5] blends. In *Figure 11* we have also reported the variation of the volume-average diameter d_v *versus* volume fraction of the minor phase; it can be considered that in this range of volume fraction, the polydispersity index d_v/d_n is about 1.3.

Newtonian viscosity

As we did for pure polymers, we have determined the zero shear viscosity of the blends from measurements carried out in steady shear at low shear rate, as well as in the oscillatory mode, in the range of linear viscoelasticity. The Cox–Merz relation is verified for all the blends studied, as shown in *Figure 13* for the 70/30 PE/PA12 blend.

For all the blends, one can observe a zero shear plateau for the viscosity, and the shear rate value at which nonlinear shear thinning effects appear decreases with increasing volume fraction of the minor phase, at least in the case of a nodular morphology. This last result is related to an increase of hydrodynamic interactions when inter-nodular distance decreases with increasing volume fraction of the minor phase, as suggested by our morphological observations. However, we cannot ignore a possible earlier deformation of the nodules when they increase in size, and hence a possible orientation in the flow field. It is expected that zero shear viscosity depends on rheological properties of the components, interfacial tension and morphology, i.e. on volume fraction, size and size-distribution of the nodules. *Figure 14* shows the dependence of zero shear viscosity (η_0) on composition for PE/PA12 blends. This figure indicates two main points: first, as a whole, η_0 values are above the straight line joining the viscosity values of the two constituents, clearly showing a positive deviation from a simple additive law[8]; and second, we observe two types of dependence of η_0 with the volume fraction, that is a monotonie increase in viscosity in regions 1 and 3 (nodular morphology) and an almost constant viscosity in region 2 (fibrillar morphology).

Dilute or semi-dilute emulsion models have been used to describe the behaviour of immiscible polymers under low deformation rate: dilute emulsion of Newtonian spheres in a Newtonian matrix, neglecting the influence of the interphase, in Taylor's model[9]; emulsion of two Newtonian
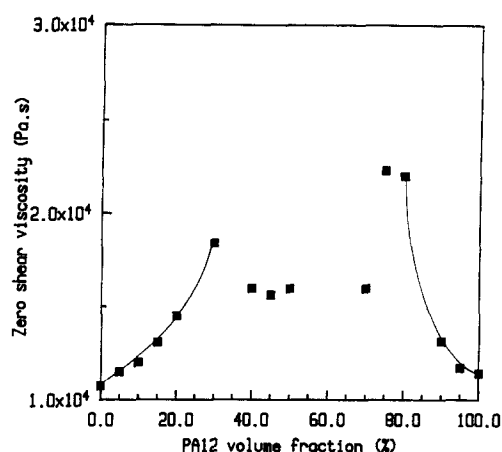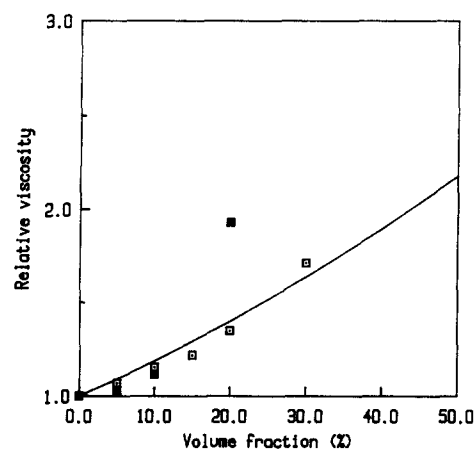

Figure 15 Variation of relative viscosity *versus* volume fraction of the minor phase. Experimental data: PE matrix (□) and PA12 matrix (■); Oldroyd's model predictions for $k = 1$ (————)

liquids with interphase characterized by the interfacial tension in Oldroyd's[10] or Choi and Schowalter's[11] models; emulsion of two viscoelastic materials in Palierne's model[12]. In most cases, these different models lead to very similar expressions between relative viscosity η_r, defined as the ratio of emulsion viscosity to that of the medium, and volume fraction Φ in the limit of not too high fractions. Only a parameter k, which is the ratio of zero shear viscosity of the dispersed phase to that of the matrix, appears in these expressions. In the case of Oldroyd's model, the relative viscosity is expressed as:

$$\eta_r = 1 + k_1\Phi + k_2\Phi^2 \qquad (1)$$

where the coefficients k_1 and k_2 are given by the following expressions:

$$k_1 = (5k + 2)/2(k + 1) \qquad (2)$$

and

$$k_2 = (5k + 2)^2/10(k + 1)^2 \qquad (3)$$

In *Figure 15*, we have compared our experimental data to model predictions for $k = 1$. A rather good qualitative agreement is observed at the lower volume fractions, although the theoretical model slightly overestimates the relative viscosity. This difference can be attributed to the polydispersity in the size of the nodules[13]. However, it is to

be noticed that for both dispersions (PE/PA12 and PA12/PE), experimental nonlinear effects with increased volume fraction appear earlier and are of higher amplitude than those predicted by the models. This is quite obvious in the case of PE dispersion in PA12. There are at least two reasons for the poor agreement between model predictions and experimental data. First, the model only takes into account hydrodynamic interactions between neighbouring drops, so neglecting other possible types of interaction such as contact interaction. Second, the model does not include any effect of particle–matrix interactions, for example in terms of surface tension between the two phases, in the limit of zero shear rate. The more limited extent of region 3 with respect to region 2, and also the more rapid increase of viscosity in region 3 are consistent with this analysis and our morphological observations.

Figure 14 shows that in the partially fibrillar region (region 2), the zero shear viscosity remains almost constant, although nearly 1.5 times higher than that of the components (of same viscosity), which was expected on the basis of a stratified (laminar) morphology following the additivity law of fluidities $(1/\eta_{blend} = \Phi_{dispersion}/\eta_{dispersion} + \Phi_{matrix}/\eta_{matrix})$. From the observation that filaments and nodules coexist in region 2, the observed viscosity excess may be qualitatively explained on the basis of recent modification of the previous model by Tsakalos[14]. In this model, the blend is assumed to be a two-phase layer system, in which one phase is of fibre type (Φ_{fibre}) whereas the other is an emulsion of dispersed phase (nodular) in the matrix ($\Phi_{emulsion}$); viscosity is then calculated by using the fluidity additivity rule. We used this model, not in order to calculate the blend's viscosity, but rather to estimate Φ_{fibre} and $\Phi_{emulsion}$ from the experimental value of the viscosity. As an example, for the 55/45 PE/PA12 blend, the model gives the following distribution: 60% fibres and 40% nodules. This result is in rather good agreement with observation of the photograph shown in *Figure 9*.

Linear viscoelasticity

Many experimental studies have been made on the linear viscoelastic behaviour of incompatible polymer blends. It is generally observed that this behaviour is characterized by an additional relaxation process at low frequencies, due to the dispersed phase deformation during oscillatory shear[15]. One striking point shown by these experiments is the development of high elasticity at low frequencies induced by the surface tension[16]. Theoretically, the above mentioned emulsion models can describe this behaviour; the interfacial contribution to the complex modulus appears as a stress of magnitude α/R which tends to minimize the surface energy, α being the interfacial tension and R the radius of dispersed particles which are assumed to be spheres.

Dynamic moduli G' and G'' have been measured, for all the volume fractions used, in the same conditions as for pure polymers. Results show that, as far as the terminal zone is concerned, the elastic modulus G' increases with the dispersed phase content. Yet the elastic modulus is clearly higher than each of the pure components, only when the volume fraction of the dispersed phase is above 20%, as shown in *Figure 16a* and *b*. Moreover, the shoulder in the G' curve[16] related to the relaxation process of nodules, clearly appears in this range of volume fraction only. This latter result, added to the necessity for the dispersion to be of nodular type, sets a limit to volume fractions that can be used for comparison with model predictions. This comparison was carried out using Palierne's model[12], in which
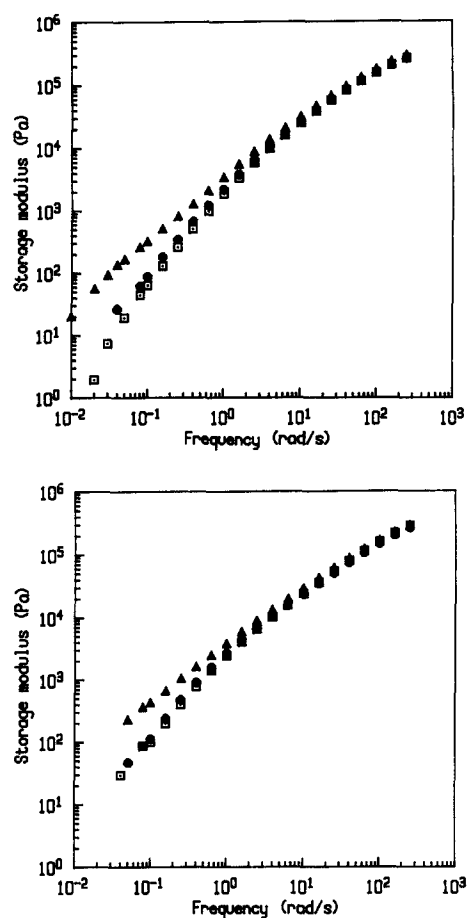

Figure 16 (a) The storage modulus as a function of the frequency. Comparison between PE (□) and 95/5 (•), 70/30 (▲) PE/PA12 blends. (b) The storage modulus as a function of the frequency. Comparison between PA12 (□) and 5/95 (•), 20/80 (▲) PE/PA12 blends

the viscoelasticity of the components, the interfacial tension and the droplet size distribution are taken into account. The interfacial tension can be determined by fitting the dynamic moduli to this model, provided that the droplet radius is known. We used a simplified version of this model proposed by Graebling *et al.*[17], by assuming that the interfacial tension is independent of local shear deformation and of variation of interfacial surface and that the droplet radius distribution can be substituted by the volume average radius R_v, when the polydispersity index does not exceed a value of about 2.3.

Figure 17 shows an example of a fit to Palierne's model for the 70/30 PE/PA12 blend. The agreement between measurements and model curves is quite good. This fit leads to a value for the α/R ratio; given $R_v = 1.5 \mu m$, we obtain $\alpha = 0.012 \text{ N m}^{-1}$. This value, confirmed by a fit for the 80/20 PE/PA12 blend, is close to the values obtained by Luciani[6] for PE/PA11 blends, using a Rayleigh instability method. In the case of the 20/80 PE/PA12 blend (PE dispersion in PA12), the agreement between experimental data and model is quite poor for any value of α/R, despite the fact that the elastic modulus is well above those of the components. The fact that the theory only takes into account hydrodynamic interactions between droplets may explain this poor agreement, when taken in relation to similar arguments to those proposed previously to explain the volume fraction dependence of zero shear viscosity in the case of dispersion of PE in a PA12 matrix.
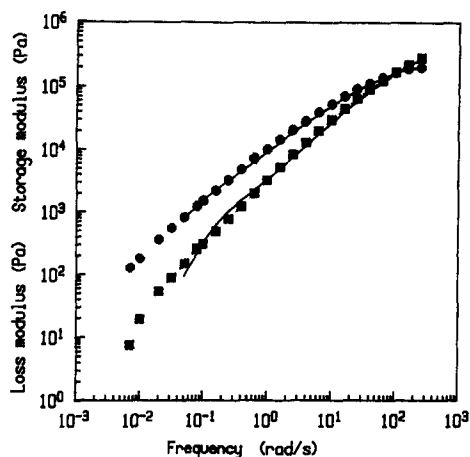
Figure 17 Frequency dependence of loss modulus (•) and storage modulus (■) for 70/30 PE/PA12 blend. Palierne's model predictions (————————) with $\alpha = 12$ mN m^{-1} and $R_v = 1.5$ μm

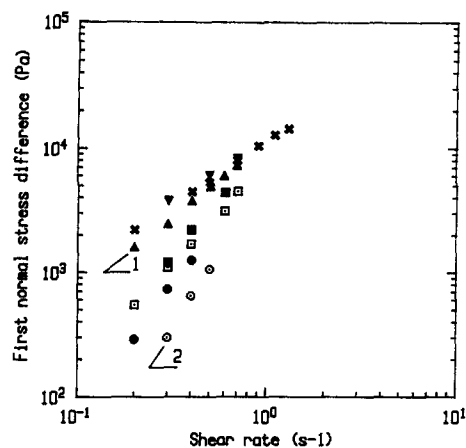**Figure 18** Variation of first normal stress difference with shear rate: PE (□); PA12 (○); 95/5 PE/PA12 blend (■); 5/95 PE/PA12 blend (•); 70/30 PE/PA12 blend (▲); 20/80 PE/PA12 blend (▼) and 50/50 PE/PA12 blend (×)

First normal stress difference

Steady shear measurements of the first normal stress difference N_1 can only be performed over a limited shear rate range of approximately one decade $(0.1$ s$^{-1} < \dot{\gamma} < 1$ s$^{-1})$. The lower limit of this range is related to the normal force threshold detection of the rheometer, whereas the upper limit is determined by the onset of flow instabilities. This upper limit seems to depend on volume fraction and hence on the blend's morphology. For example, the highest shear rate obtained, about 1.5 s^{-1}, corresponds to a 50/50 blend with fibrillar morphology. Moreover this upper limit is higher than shear rates above which the non-Newtonian flow of blends begins; so, in contrast with previous data obtained in the linear viscoelastic range, we cannot ignore a possible change of blend structure in these experiments. Since the droplets for the blends used in this study are treated as spheres in the Newtonian range, at least in regions 1 and 3, we have examined the possibility of deformation of droplets in the shear rate range of interest. The droplet deformation is calculated by applying the theory of Taylor[18] for an isolated droplet; the deformation parameter D is:

$$D = \frac{a-b}{a+b} \tag{4}$$

where a and b are respectively the major and the minor axes of the ellipsoidal droplet. D is expressed as:

$$D = C_a \frac{19k + 16}{16k + 16} \tag{5}$$

where C_a is the capillary number

$$C_a = \frac{\eta_M \dot{\gamma} R}{\alpha} \tag{6}$$

with η_M being the matrix viscosity.

In general, the droplet is regarded as deformed when D exceeds 0.05 and will be broken by shear forces when D is higher than 0.5.

According to these criteria, we can conclude that, in the shear rate range used to measure normal forces, the droplets are deformed whatever the volume fraction; for instance D is 0.07 for $\Phi(PA12) = 5\%$ at $\dot{\gamma} = 0.2$ s^{-1}, which is the least likely case. Moreover, except for the lowest volume fractions of the dispersed phase, break-up of droplets is expected $(D = 1.5$ for $\Phi(PA12) = 30\%$ and $D = 1.7$ for $\Phi(PE) = 20\%$ at $\dot{\gamma} = 1$ s$^{-1})$. Notice that the expression
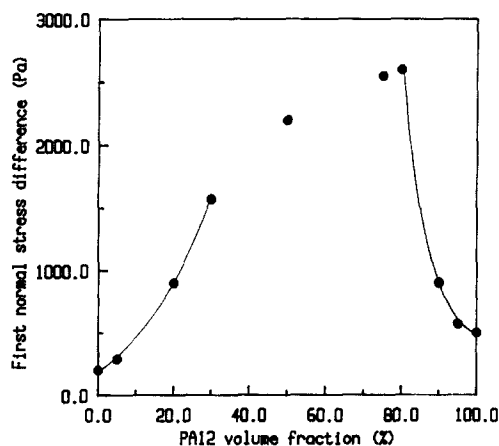

Figure 19 Volume fraction dependence of the first normal stress difference measured at $\dot{\gamma} = 0.2$ s^{-1}, for PE/PA12 blends

derived by Choi and Schowalter[10] for the deformation of Newtonian droplets in a Newtonian matrix, taking into account the volume fraction of the dispersed phase, leads to the same conclusions.

Figure 18 shows the variation of first normal stress difference N_1 with the shear rate for only some volume fractions, for the sake of clarity. For all blends studied, it can be observed that:

• As for the constituents, N_1 is proportional to shear rate squared for blends having a low volume fraction of the minor phase, i.e. $\Phi(PA12)$ and $\Phi(PE)$ equal to 5%.
• On the other hand, for all the other blends, N_1 is almost proportional to the shear rate.

By considering that the blend morphology is affected during normal stress difference measurement, as shown above, this last result can be related to the predictions of the model developed by Doi and Ohta[19] for a 1/1 blend of two immiscible Newtonian fluids having the same viscosity. In this model, the viscoelastic behaviour results from additional stresses generated during flow due to interfacial tension; these stresses change with deformation and relaxation of the interface, i.e. with deformation, break-up and aggregation of droplets during flow. The Doi–Ohta theory predicts that the zero shear viscosity is independent

of shear rate, while the first normal stress difference is proportional to the shear rate, as observed experimentally by Takahashi *et al.*[20]. Since all the parameters required to use Doi–Ohta theory are not available through our experiments, we cannot at this stage further compare theory and experiments as Guenther and Baird[21] have done recently.

Figure 19 shows the composition dependence of the first normal stress difference measured at $\dot{\gamma} = 0.2\ \text{s}^{-1}$. These results clearly show a positive deviation from a simple additivity rule, where only the first normal stress difference of the constituents would contribute. It can be seen that N_1 increases gradually at low and moderate volume fraction of the dispersed phase (regions 1 and 3), although this increase, as for zero shear viscosity, is more rapid in region 3 than in region 1. On the other hand, *Figure 19* also shows that in the phase inversion region (region 2), the N_1 values, which are similar to those obtained at the limit of region 1 and 3, seem relatively insensitive to the volume fraction.

CONCLUSION

The investigation reported herein has enabled us to correlate, at least qualitatively, morphology and rheological properties of blends of two immiscible polymers having almost the same viscosity but different elasticity, over a wide range of composition.

In relation with the morphology of blends observed at rest, the composition dependence of the zero shear viscosity can be explained with an emulsion model at low and moderate volume fraction in the case of droplet-type morphology, whereas the dependence at intermediate volume fraction is analysed on the basis of a model of additivity of component's fluidity, taking into account the simultaneous presence of droplets and fibres.

The analysis of small amplitude dynamic measurements is based on Palierne's model and the interfacial tension can be estimated. However, the volume fraction range of applicability of this model is rather limited for the blends investigated in this study.

Except for the lowest volume fractions of dispersed phase, the first normal stress difference is almost proportional to the shear rate as predicted by the Doi–Ohta theory. This behaviour is attributed to a modification of the blend morphology in a flow field. On the other hand, the composition dependence of N_1 shows a positive deviation from an additivity rule.

Moreover, we can note that the dissymetry observed for the variation of the droplet size with volume fraction, at low and moderate concentration of dispersed phase, is also shown by $\eta_0 - \Phi$ and $N_1 - \Phi$ dependence and may be due to the relative elasticity of the components. It would thus be interesting to confirm this feature by varying the elasticity of the blend components.

REFERENCES

1. Utracki, L. A., *Polymer Alloys and Blends*, Hanser Publishers, New York, 1990.
2. Yoshida, M., Ma, J. J., Min, K., White, J. L. and Quirk, R. P., *Polym. Eng. Sci.*, 1990, **30**, 30.
3. Subramanian, P. M., *Polym. Eng. Sci.*, 1985, **25**(8), 483.
4. Heinkens, D. and Barentsen, W., *Polymer*, 1977, **18**, 69.
5. Favis, B. D. and Chalifoux, J. P., *Polymer*, 1988, **29**, 1761.
6. Luciani, A., Establishment mechanism of morphologies in immiscible polymer blends, Thesis, Université Pierre et Marie Curie, Paris VI, Editions Technip, Paris, France, 1993.
7. Starita, J. M., *Trans. Soc. Rheol.*, 1972, **16**, 339.
8. Utracki, L. A., *J. Rheol.*, 1991, **35**(8), 1615.
9. Taylor, G. I., *Proc. Roy. Soc.*, 1932, **A138**, 41.
10. Oldroyd, J. G., *Proc. Roy. Soc.*, 1955, **A232**, 567.
11. Choi, S. J. and Schowalter, W. R., *Phys. of Fluids*, 1975, **18**, 420.
12. Palierne, J. F., *Rheologica Acta*, 1990, **29**, 204.
13. Goto, H. and Kuno, H., *J. Rheol.*, 1982, **26**, 387.
14. Tsakalos, V., Establishment mechanism of morphologies for polymer blends in simple shear – Relation with rheological behaviour, Thesis, Ecole Nationale Superieure des Olives de Paris, Sophia-Antipolis, France, 1995.
15. Bousmina, M. and Muller, R., *J. Rheol.*, 1993, **37**, 663.
16. Graebling, D., Muller, R. and Palierne, J. F., *Macromolecules*, 1993, **26**, 320.
17. Graebling, D., Benkira, A., Gallot, Y. and Muller, R., *Eur. Polym. J.*, 1994, **30**, 301.
18. Taylor, G. I., *Proc. Roy. Soc.*, 1934, **A146**, 501.
19. Doi, M. and Ohta, T., *J. Chem. Phys*, 1991, **95**(2), 1242.
20. Takahashi, Y., Kurashima, N. and Noda, I., *J. Rheol.*, 1994, **38**(3), 699.
21. Guenther, G. K. and Baird, D. G., *J. Rheol.*, 1996, **40**, 1.